International Journal of Mass Spectrometry 272 (2008) 172–179

Contents lists available at ScienceDirect

International Journal of Mass Spectrometry

journal homepage: www.elsevier.com/locate/ijms

Parity alternation of linear ground-state hydrogenated cationic carbon clusters HC_nSi^+ (n = 1–10)

J. Yang [a], J.Y. Qi [a], J. Liu [a,1], M.D. Chen [a,*], Q.E. Zhang [a], C.T. Au [b]

[a] State Key Laboratory of Physics Chemistry of Solid Surfaces, Department of Chemistry, Center for Theoretical Chemistry, College of Chemistry and Chemical Engineering, Xiamen University, Xiamen 361005, People's Republic of China
[b] Department of Chemistry, Hong Kong Baptist University, Kowloon Tong, Hong Kong, People's Republic of China

ARTICLE INFO

Article history:
Received 18 December 2007
Received in revised form 6 February 2008
Accepted 13 February 2008
Available online 10 March 2008

Keywords:
Triatomic cluster
Cation
HC_nSi^+
Silicon-doped cluster
Density functional study

ABSTRACT

Making use of molecular graphics software, we have designed numerous models of HC_nSi^+ (n = 1–10), and by means of the B3LYP density functional method, performed geometry optimization and calculation on vibrational frequency. The ground-state isomers of HC_nSi^+ (n = 1–10) are found to be linear with the Si and H atom located at the ends of the C_n chain. When n is even, the C_n chain is polyacetylene-like whereas when n is odd, the C_n chain displays a structure that fades into a cumulenic-like arrangement towards the Si end. According to the results of mass spectrometric investigation available in the literature, the intensities of even-n HC_nSi^+ are more intense than those of odd-n HC_nSi^+, implying that the former are more stable than the latter. We detect trends of odd/even alternation in electronic configuration, the highest vibrational frequency, ionization potential, incremental binding energy as well as in certain bond length and certain atomic charge of the linear ground-state structures of the HC_nSi^+ (n = 1–10) clusters. The calculation results reveal that the even-n cationic clusters are more stable than the odd-n ones.

1. Introduction

The research on the structures and properties of small carbon clusters has a long history [1]. In the last decade, carbon clusters doped with heteroatom(s) have attracted immense attention. It is of fundamental significance to compare the reactivity of carbon clusters with that of the doped counterparts. Carbon chains doped with heteroatom(s) are also important in astrophysics. A variety of carbon clusters bonded to heteroatom(s) such as O, N, S, and Si have been observed in interstellar clouds. The UMIST database for astrochemistry stores thousands of gas-phase reactions that are important in astrophysical environments, and the species involved in their hundreds [2]. As described by Millar, species belong to the polyynes series have been detected in circumstellar environment of late-type carbon-rich stars (such as star IRC +10216), and in dense and dark interstellar molecular clouds (such as TMC-1) as well as in hot molecular cores [3]. In recent years, carbon chains and rings which are of astrophysical interest have been identified in supersonic molecular beams by means of Fourier-transform microwave and laser cavity ring down spectroscopy [4,5]. Silicon is a major constituent of interstellar dust, and silicon-doped carbon clusters are fairly abundant in certain interstellar and circumstellar sources [6]. In laser ablation of graphite targets and arcing across graphite electrodes in ammonia, compounds belonging to the polyynes series were generated [7]. Using a mixture of silicon carbide and polycyclic aromatic compounds as a target for laser ablation, Huang et al. generated clusters ions composed of carbon and silicon atoms and a single hydrogen atom [8].

Despite the intriguing findings, theoretical investigations on hetero-carbon triatomic clusters are not that many. Using a large-scale coupled cluster method, Botschwina et al. conducted investigations on HC_5N, HC_5NH, HC_4NC, HC_5NC, HC_6NC, and HC_9NH^+ [9–12]. High-level coupled cluster calculations on theoretical structures of the carbine HC_4N and NC_nS (n = 1–7) were carried out by McCarthy et al. [13,14]. Scemama et al. examined the structures and properties of polyynes $HC_{2n}H$ (n = 1–8) and cyanopolyynes $HC_{2n-1}N$ (n = 1–7) by density functional calculations [15]. Using the B3LYP density functional method, Allamandola et al. investigated the geometries and harmonic frequencies of hydrogenated cyanopolyyne $HC_{2n+1}N$, (n = 0–5) species [16]. By means of ab initio calculations, Liu et al. examined structures of HC_nS^+ (n = 3–13) and HC_nS^- (n = 4–18) [17] while Flores studied the electronic spectra of SC_nH radicals (n = 2–4) [18].

The time-of-flight mass spectra of $HSiC_n^+$ clusters show an abundance pattern of odd/even alternation: the even-n clusters are more prominent than the odd-n ones [8]. To the best of our knowledge, there are no systematic theoretical studies on

DOI of original article: 10.1016/j.ijms.2007.12.004.
* Corresponding author. Tel.: +86 592 2182332; fax: +86 592 2184708.
E-mail address: mdchen@xmu.edu.cn (M.D. Chen).
[1] Present address: Department of Chemistry, The Chinese University of Hong Kong, Shatin, Hong Kong, People's Republic of China.

1387-3806/$ – see front matter © 2008 Elsevier B.V. All rights reserved.
doi: 10.1016/j.ijms.2008.02.010

small $HSiC_n^+$ clusters. To explore the experimental observation theoretically, we designed a huge number of structural models of HC_nSi^+ (n = 1–10), and performed geometry optimizations and calculations on vibrational frequencies by means of the B3LYP density functional method in this study. The geometry structure, bonding character, atomic charge, electronic configuration, the highest vibrational frequency, ionization potentials, incremental binding energy, and dissociation channels of the linear ground-state clusters were examined. Based on the results, we provide explanation on why the even-n HC_nSi^+ (n = 1–10) isomers are more stable than the odd-n ones. The outcomes can serve as a guideline for the synthesis of similar kind of materials as well as for future theoretical studies on heteroatom(s)-doped carbon clusters which are so commonly found in circumstellar environments.

2. Computational method

During the investigation, devices for molecular graphics, molecular mechanics, and quantum chemistry were used. To start, a three-dimensional model of a cluster was designed using HyperChem for Windows [19] and Desktop Molecular Modeller [20] on a PC computer. The model was optimized by MM+ molecular mechanics and semi-empirical PM3 quantum chemistry. Then, geometry optimization and calculation of vibrational frequencies were conducted using the B3LYP density functional method of Gaussian 03 package [21] with 6–311G** basis sets, i.e., Becke's 3-parameter nonlocal exchange functional with the correlation functional of Lee–Yang–Parr [22,23]. It has been pointed out that geometries computed with more expensive basis sets do not necessarily lead to more accurate final results [24]. The single point energy calculations following the optimizations were performed using the larger 6–311+G** basis set (i.e., B3LYP/6–311 + G**//B3LYP/6–311G**). Because the change of zero point energy (ZPE) could only be affected slightly by the quality of the employed method, all energies were calculated with ZPE correction at the B3LYP/6–311G** level. The optimized models were again displayed using HyperChem for Windows. The data of partial charges and bond orders were explored with Gaussian natural bond orbital (NBO). All of the calculations were carried out on the servers of SGI.

3. Results and discussion

3.1. Geometry configuration

Because there are so many possible structures of the clusters, the identification of the ground-state isomers is important. For a particular family of molecules, the basic structure with the lowest energy affects the "building" of larger molecules. The ground-state isomers of heteroatom(s)-doped carbon clusters may adopt different configurations. The linear configurations terminated by the heteroatom(s) are rather popular among the most stable isomers, e.g., C_nN^- (n = 1–7) [25]. For the boron-doped carbon clusters C_nB (n = 4–10) [26] and beryllium-doped carbon dianion clusters C_nBe^{2-} (n = 4–14) [27], the linear configuration with the boron and beryllium atoms located inside the carbon chain are the most stable isomers. For C_nH^- ($n \leq 10$) clusters, the configurations with a bent C_n chain terminated by the hydrogen atom are the most favorable in energy [28]. In the cases of CsC_7^-, CsC_9^-, and $TiC_n^{+/-}$ (n = 1–6) clusters isomers with a "lightly embracing" or "fan" structure have been suggested to be the most stable [29,30].

At the beginning of our investigation, nothing was known other than the HC_nSi^+ formula. The assumption of a reasonable geometrical structure was the initial step. Unfortunately, there is no experimental technique that can provide direct information on cluster geometry. The only method that enables the determination of cluster geometries at present is based on comparing the total energy after theoretical calculations. In order to locate the global minimum on an energy surface, it is necessary to investigate a large number of models; otherwise the structure with the lowest energy may be missed. In order to reduce the chance of having the ground-state structures wrongly determined, we examined a huge number of models which are reasonable in chemical understandings. After geometry optimization, the total energies were compared for the identification of ground-state isomers. For models with imaginary vibrational frequencies and/or of higher energies, they were discarded.

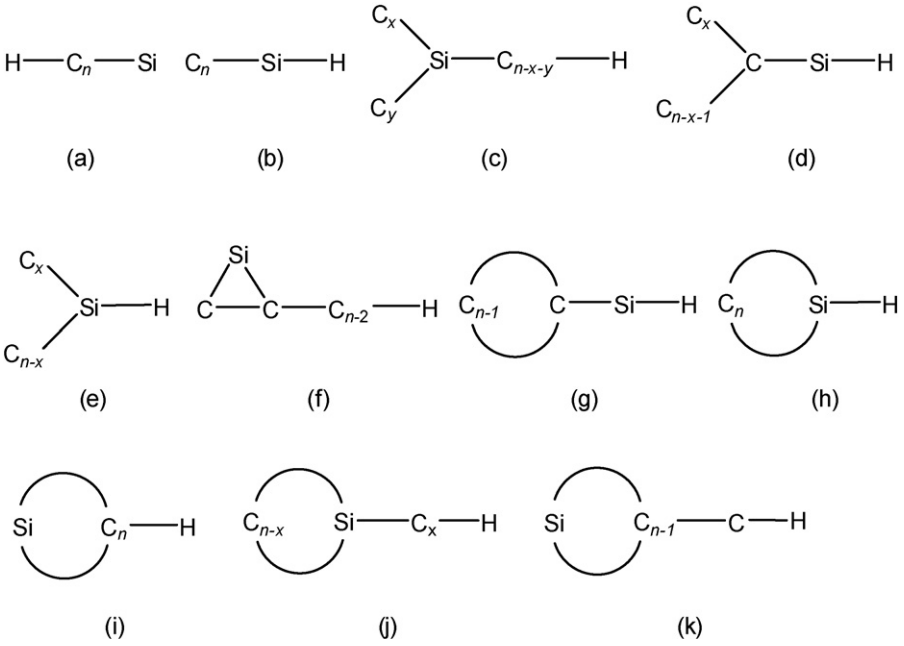

Fig. 1. Eleven main categories of HC_nSi^+ (n = 1–10) structures (x, y denote numbers of carbon atom(s)).

Eleven major categories of HC_nSi^+ (n = 1–10) structures are displayed in Fig. 1. Belonging to category 1a are isomers of linear structures, the Si and H atom are located at the ends of a C_n chain. Belonging to category 1b are linear isomers with a −SiH unit bonded to one end of a C_n chain. The isomers of category 1c are "Y" shaped with the Si atom bonded to three carbon branches, and the H atom located at the end of one of the branches. The isomers of category 1d are with a C atom bonded to two carbon branches and a −SiH unit simultaneously whereas those of category 1e are with the Si atom bonded to the H atom and two carbon branches. Category 1f show a C_2Si ring connected to a $C_{n-2}H$ chain via a C—C bond. Belong to category 1g are isomers with a −SiH unit bonded to an atom of a C_n ring. In category 1h are isomers with the H atom bonded to the Si atom of a C_nSi ring, whereas in category 1i, the isomers are with the H atom bonded to a carbon atom of a C_nSi ring. The isomers of category 1j are isomers with a $-C_xH$ chain bonded to the Si atom of a SiC_{n-x} ring. The isomers of category 1k are isomers with a −CH unit bonded to a C atom of a SiC_{n-1} ring. After looking into a large number of models, we determined that the linear HC_nSi^+ (n = 1–10) clusters of category 1a are the linear ground-state isomers except the particular case of HC_3Si^+.

Flores et al. carried out an ab initio study of SiC_2 protonation [31]. An ab initio theoretical study of the $(SiC_2H_2)^+$ species has been carried out by Largo and Barrientos [32]. They showed that the ground-state of HC_2Si^+ is linear. Redondo et al. conducted theoretical study of $(SiC_3H)^+$ and $(SiC_3H_2)^+$ species based on MP4 at MP2 geometries and QCISD(T) at B3LYP geometries [33]. At the B3LYP level the linear isomer is predicted to be the lowest-lying species. However, other high-level ab initio methods (e.g., QCISD(T), PMP4) suggested that the global minimum is a cyclic isomer derived from protonation of ground-state rhomboidal C_3Si, with the linear isomer (the second most stable structure) lying about 4–6 kcal/mol higher in energy. It has been considered that the QCISD(T) results of $HSiC_3^+$ could be more reliable than the B3LYP ones [33]. In our study we performed systematic study on the parity alternation of HC_nSi^+ species. We consider that the B3LYP method is an affordable level for qualitative analysis of HC_nSi^+ clusters.

3.2. Bond characters

Displayed in Fig. 2 are the bond lengths and NBO charges of the linear ground-state HC_nSi^+ (n = 1–10) clusters (category 1a). One can see that the H–C and C–Si lengths are within the 1.067–1.088 Å and 1.738–1.797 Å range, respectively, exhibiting essentially the characteristic of single bond. With n = 3–10, the C—Si bond lengths of the even-n HC_nSi^+ are shorter than those of the neighboring odd-n counterparts, exhibiting a pattern of long/short alternation (Fig. 3). Shown in Fig. 4 are the plots of (H)C—C and C—C(Si) bond lengths of the linear ground-state HC_nSi^+ (n = 2–10) clusters versus the number of carbon atoms (n). One can see patterns of odd/even alternation: the (H)C—C and C—C(Si) bond lengths of the odd-n clusters are longer than those of the even-n ones, and the extent of alternation of the former is smaller than that of the latter. The bonding of small linear carbon chains could be either cumulene- or polyacetylene-like [34]. Along the chains of the linear ground-state HC_nSi^+ (n = 3–10) structures, the length of the C—C bonds also show an alternate short/long pattern. When n is even, the C—C bonds display a typical polyacetylene-like character, i.e., a series of alternate

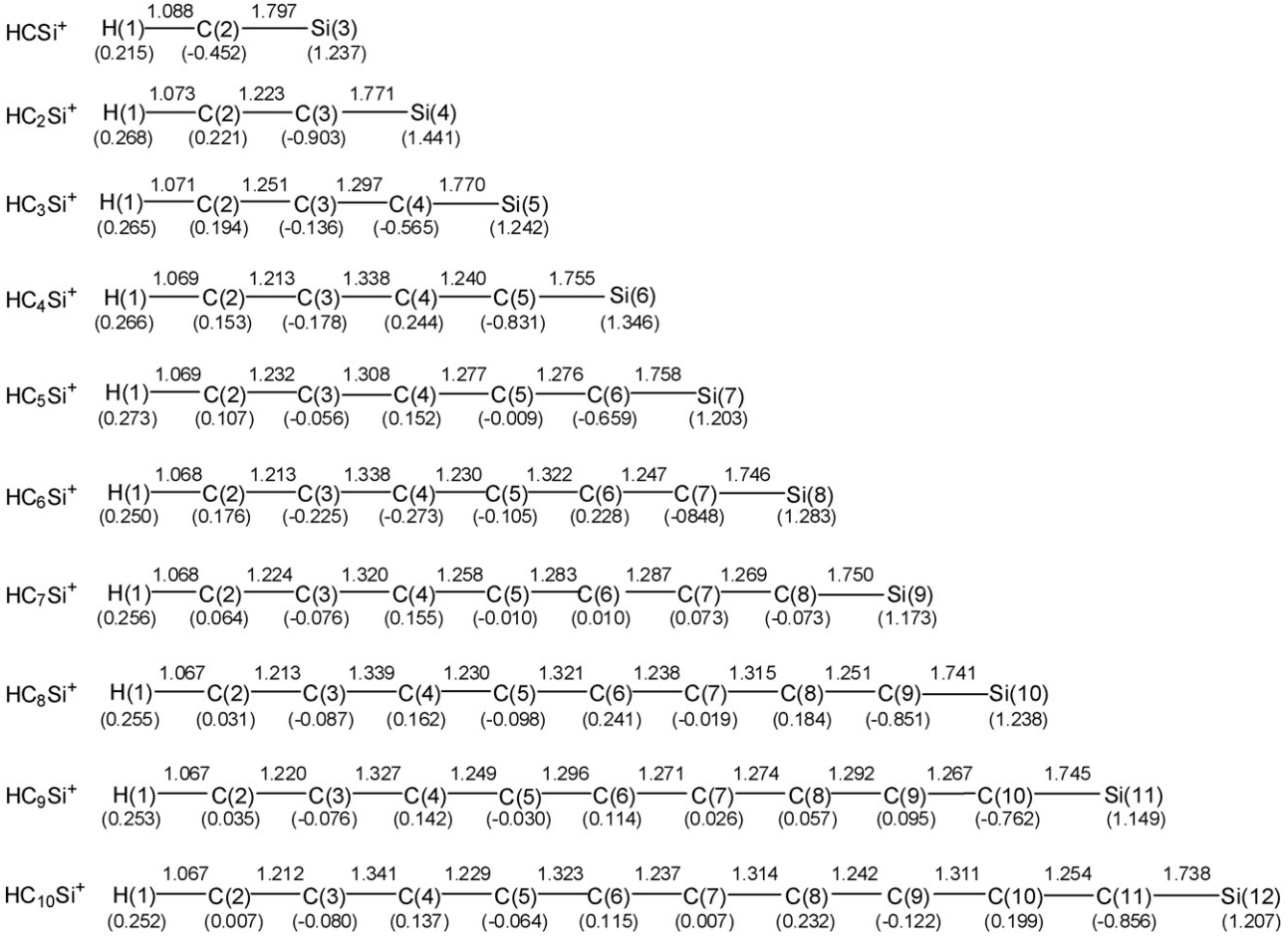

Fig. 2. Bond lengths (Å) and NBO charges (in parentheses) of the linear ground-state HC_nSi^+ (n = 1–10) clusters.

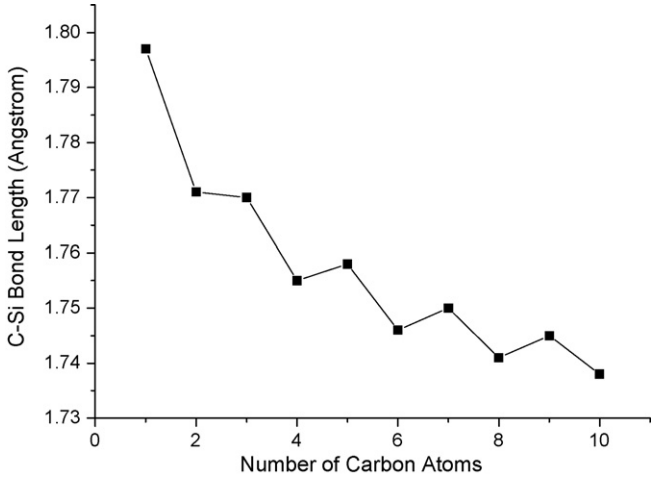

Fig. 3. C—Si bond lengths (in Å) of ground-state HC_nSi^+ (n = 1–10) versus the number of carbon atoms (n).

single and triple bonds marked with a regular alternation of long (~1.311–1.341 Å) and short (~1.212–1.254 Å) bonds. When n is odd, the pattern of short/long alternation of C—C bond lengths fades out gradually from the H end to the Si end, and the C—C bonds close to the Si terminus tend to even out in lengths, and exhibit some sort of cumulenic character (with consecutive double bonds having bond lengths of ~1.249–1.297 Å). As an illustration, depicted in Fig. 5 are the bond lengths of the linear ground-state HC_9Si^+ and $HC_{10}Si^+$ clusters versus the number of bond (as counted from the left in Fig. 1, e.g., the H—C bond length is plotted against "1" and so on). The curve of the $HC_{10}Si^+$ with polyacetylene-like carbon chain displays the pattern of short/long alternation. As for HC_9Si^+, the carbon chain is cumulene-like along the side close to the Si terminus. The results of Gaussian NBO based on natural bond orbitals analysis corroborate the above characteristics of bonding. Both H—C bond and C—Si bond are single bond. When n is even, the C—C bonds display alternate single and triple bonds (i.e., polyacetylene-like). When n is odd, the C—C bonds close to the H terminus displays triple bond characters, whereas getting close to the Si terminus the C—C bonds appear as consecutive double bonds (i.e., getting cumulenic-like).

Also displayed in Fig. 2 are the NBO atomic charges (values in parentheses underneath the atoms) of the linear ground-state

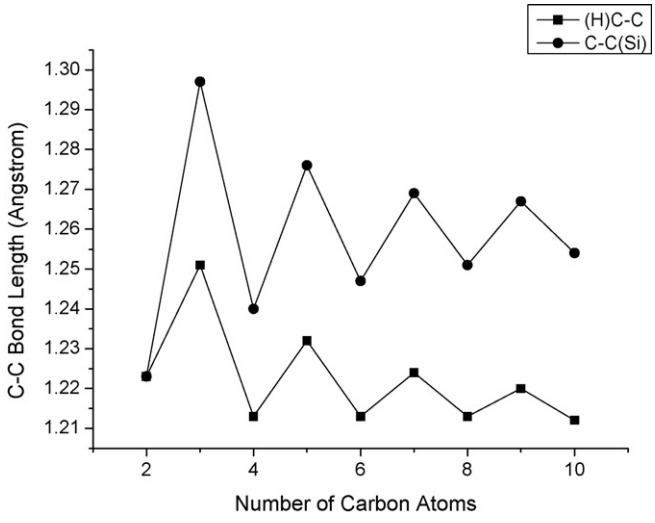

Fig. 4. Lengths of the C—C bond next to H and Si atom (in Å) of the linear ground-state HC_nSi^+ (n = 2–10) clusters versus the number of carbon atoms (n).

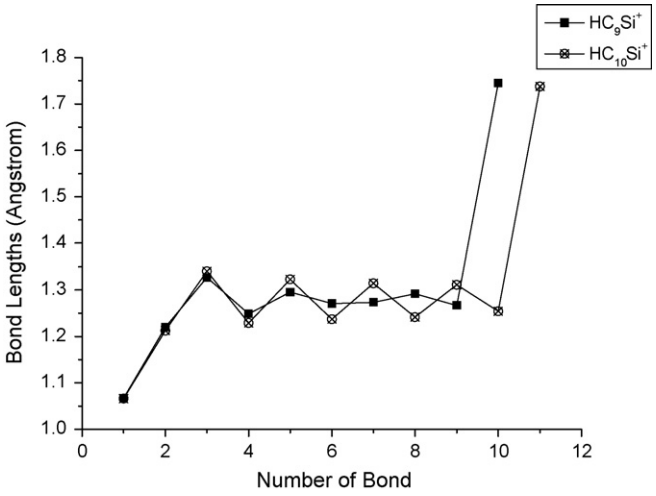

Fig. 5. Bond lengths (in Å) of the linear ground-state HC_9Si^+ and $HC_{10}Si^+$ clusters versus the number of bond (as counted from the left in Fig. 2).

HC_nSi^+ (n = 1–10) clusters. The levels of positive charge on the Si and H atom are relatively higher than that on the C atoms. Shown in Fig. 6 is a plot of the positive charges on silicon atom of the linear ground-state HC_nSi^+ (n = 1–10) clusters versus the number of carbon atoms (n). The level of positive charges (in the range of 1.149–1.441) on the silicon atoms decreases with a rise in n, showing a sort of odd/even alternation. The positive charge on the silicon atom of an even-n cluster is larger than that of the neighboring odd-n ones. The positive charge of the hydrogen atoms are in the range of 0.215–0.273, and the charges located on the carbon atoms could be considered as minor.

3.3. Electronic configuration and valence-bond structures

The electronic configurations of linear ground-state HC_nSi^+ (n = 2–10) clusters are similar to those of C_nSi clusters [35] and can be summarized as

$$(\text{core})1\sigma^2 \ldots 1\pi^4 \ldots (n+2)\sigma^2 \ldots \left(\frac{n+1}{2}\right)\pi^2 \quad n \text{ is odd}$$

$$(\text{core})1\sigma^2 \ldots 1\pi^4 \ldots (n+2)\sigma^2 \ldots \left(\frac{n}{2}\right)\pi^2 \quad n \text{ is even}$$

The HC_nSi^+ (n = 1–10) clusters possess ($4n$ + 4) valance electrons, among which are $2n$ + 4 σ and $2n$ π electrons. When n is even, the

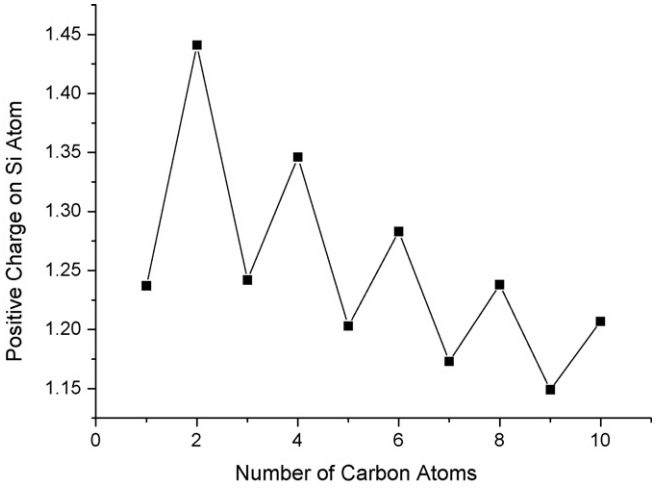

Fig. 6. Positive charges on Si atom of the linear ground-state HC_nSi^+ (n = 1–10) clusters versus the number of carbon atoms.

Table 1
Valence orbital configuration of the linear ground-state HC_nSi^+ (n = 1–10) clusters

Clusters	Configuration
$HCSi^+$	(Core) $\sigma^2\sigma^2\sigma^2\pi^2$
HC_2Si^+	(Core) $\sigma^2\sigma^2\sigma^2\sigma^2\pi^4$
HC_3Si^+	(Core) $\sigma^2\sigma^2\sigma^2\sigma^2\pi^4\sigma^2\pi^2$
HC_4Si^+	(Core) $\sigma^2\sigma^2\sigma^2\sigma^2\sigma^2\pi^4\sigma^2\pi^4$
HC_5Si^+	(Core) $\sigma^2\sigma^2\sigma^2\sigma^2\sigma^2\sigma^2\pi^4\pi^4\sigma^2\pi^2$
HC_6Si^+	(Core) $\sigma^2\sigma^2\sigma^2\sigma^2\sigma^2\sigma^2\sigma^2\pi^4\pi^4\sigma^2\pi^4$
HC_7Si^+	(Core) $\sigma^2\sigma^2\sigma^2\sigma^2\sigma^2\sigma^2\sigma^2\sigma^2\pi^4\pi^4\sigma^2\pi^4\pi^2$
HC_8Si^+	(Core) $\sigma^2\sigma^2\sigma^2\sigma^2\sigma^2\sigma^2\sigma^2\sigma^2\sigma^2\pi^4\pi^4\sigma^2\pi^4\pi^4$
HC_9Si^+	(Core) $\sigma^2\sigma^2\sigma^2\sigma^2\sigma^2\sigma^2\sigma^2\sigma^2\sigma^2\sigma^2\pi^4\pi^4\pi^4\sigma^2\pi^4\pi^2$
$HC_{10}Si^+$	(Core) $\sigma^2\sigma^2\sigma^2\sigma^2\sigma^2\sigma^2\sigma^2\sigma^2\sigma^2\sigma^2\sigma^2\pi^4\pi^4\pi^4\sigma^2\pi^4\pi^4$

outermost doubly degenerate π orbitals are fully occupied ($^1\Sigma^+$ electronic state) whereas when n is odd, they are half-filled ($^3\Sigma^-$ electronic state). The HOMO with fully filled π orbitals is energetically more stable than that with a half-filled electron shell. The alternation between $^1\Sigma^+$ (even n) and $^3\Sigma^-$ (odd n) arises from the fact that the MOs with π-symmetry are doubly degenerate. The inclusion of an extra carbon atom to a ground-state even-n HC_nSi^+ cluster would result in having two more electrons included in the π-system. The two electrons are accommodated in the π orbital, resulting in a triplet state (Table 1).

3.4. Vibrational frequencies

According to the vibrational frequencies and intensities of the linear ground-state HC_nSi^+ (n = 1–10) clusters (Table 2), the stretching modes transform as the σ irreducible representation and doubly degenerate bending modes transform as the π irreducible representation. As expected, the bending modes carry little intensity. The intensities of the stretching modes are usually much larger than those of the bending modes. The highest frequencies of the linear ground-state HC_nSi^+ clusters are 3387, 3383, 3419, 3407, 3431, 3422, 3439, 3432, and 3444 cm^{-1} for n = 2–10, respectively. Shown in Fig. 7 is a plot of the highest frequencies of the linear ground-state HC_nSi^+ (n = 2–10) clusters versus n. One can see that there is an odd/even pattern in the stretching mode of the highest frequency. The frequency of an even-n structure is larger than that of the neighboring odd-n isomers, and the value of the frequency increases with a rise in n. Similar feature was also noticed in linear C_nS (n = 2–9), SC_nS (n = 2–6), and C_nS^{2-} (n = 6–18) clusters [27,36,37]. It seems that the odd/even pattern observed for the stretching modes can be qualitatively understood based on the variation in general stability of the clusters. The clusters with even n are more stable than those with odd n, and there is bond strengthening in the structures of the former. The σ mode with the highest frequency consists mostly of the stretching motions of the bonds, this alternating pattern of σ frequency is consistent with the stability of the clusters with even n.

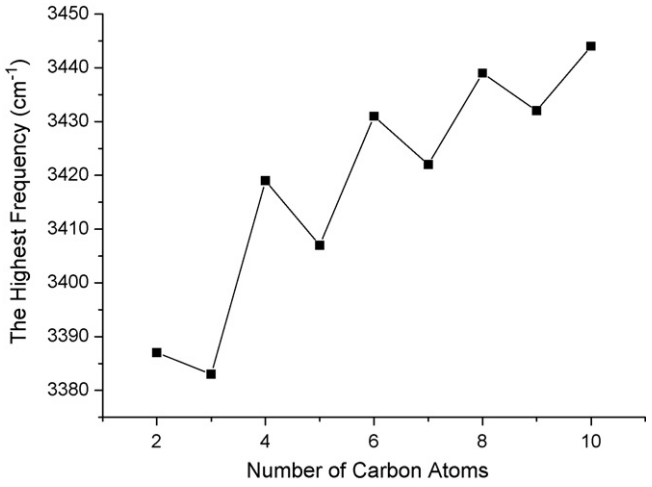

Fig. 7. The highest frequencies (cm^{-1}) of the linear ground-state linear HC_nSi^+ (n = 2–10) clusters versus the number of carbon atoms.

3.5. Ionization potentials

Listed in Table 3 are the electronic state, total energy, proton affinity (PA), ionization potential (IP), atomization energy (ΔE_a), and incremental binding energy (ΔE^I) of the linear ground-state HC_nSi^+ (n = 1–10) clusters acquired using zero point energy correction. In the case of triplet state HC_nSi^+ (n = 1–10) isomers, the spin contamination $\langle S^2\rangle$ value (before annihilation of the contaminants) stays within the 2.01–2.10 range, and such small deviation should not have severe effect on our results.

Table 2
Vibrational frequencies (cm^{-1}) and intensities (km/mol) of the linear ground-state HC_nSi^+ (n = 1–10) clusters

Clusters	Vibrational frequencies and intensities (in parentheses)
$HCSi^+$	π: 429(29), 429(29) σ: 872(54), 3199(106)
HC_2Si^+	π: 144(21), 144(21), 812(19), 812(19) σ: 710(123), 2075(531), 3387(78)
HC_3Si^+	π: 140(11), 140(11), 413(1), 413(1), 568(30), 568(30) σ: 590(69), 1420(137), 1907(22), 3383(203)
HC_4Si^+	π: 92(10), 92(10), 257(1), 257(1), 575(12), 575(12), 765(26), 765(26) σ: 542(94), 1121(130), 2072(222), 2246(1526), 3419(129)
HC_5Si^+	π: 80(7), 80(7), 202(0), 202(0), 406(7), 406(7), 556(3), 556(3), 666(27), 666(27) σ: 481(57), 951(96), 1617(90), 1928(44), 2012(371), 3407(241)
HC_6Si^+	π: 61(7), 61(7), 151(0), 151(0), 293(7), 293(7), 535(0), 535(0), 695(10), 695(10), 742(26), 742(26) σ: 443(71), 852(103), 1331(126), 2049(1044), 2198(576), 2258(2370), 3431(169)
HC_7Si^+	π: 51(5), 51(5), 130(0), 130(0), 242(6), 242(6), 409(0), 409(0), 549(4), 549(4), 683(30), 683(30), 776(1), 776(1) σ: 404(42), 758(83), 1189(109), 1701(169), 1857(43), 2032(215), 2098(809), 3422(261)
HC_8Si^+	π: 41(4), 41(4), 103(0), 103(0), 193(6), 193(6), 306(0), 306(0), 481(1), 481(1), 569(10), 569(10), 597(0), 597(0), 729(31), 729(31) σ: 373(55), 702(78), 1072(149), 1443(141), 2037(1078), 2139(3477), 2216(2808), 2269(32), 3439(207)
HC_9Si^+	π: 35(3), 35(3), 91(0), 91(0), 169(5), 169(5), 265(0), 265(0), 399(4), 399(4), 475(0), 475(0), 523(1), 523(1), 606(4), 606(4), 691(30), 691(30) σ: 346(32), 643(64), 976(136), 1331(95), 1739(67), 1780(201), 2017(871), 2106(988), 2132(323), 3432(291)
$HC_{10}Si^+$	π: 29(3), 29(3), 76(0), 76(0), 140(4), 140(4), 225(0), 225(0), 320(4), 320(4), 486(0), 486(0), 519(0), 519(0), 620(11), 620(11), 682(0), 682(0), 719(30), 719(30) σ: 320(46), 604(54), 902(155), 1218(136), 1510(144), 2019(2870), 2122(4668), 2144(4693), 2237(1), 2275(0), 3444(244)

Table 3
Electronic state, total energy (a.u.), ionization potential (IP) (a.u.), atomization energy ΔE_a (a.u.), and incremental binding energy ΔE^I (a.u.) of the linear ground-state HC_nSi^+ (n = 1–10) clusters

Cluster	State	Total energy	IP	ΔE_a	ΔE^I
$HCSi^+$	$^3\Sigma^-$	−327.75447	0.32298	0.00088	
HC_2Si^+	$^1\Sigma^+$	−365.92273	0.27031	0.31187	0.31099
HC_3Si^+	$^3\Sigma^-$	−403.97158	0.29593	0.50345	0.19158
HC_4Si^+	$^1\Sigma^+$	−442.10451	0.26099	0.77911	0.27566
HC_5Si^+	$^3\Sigma^-$	−480.16303	0.28071	0.98037	0.20125
HC_6Si^+	$^1\Sigma^+$	−518.28206	0.25455	1.24213	0.26177
HC_7Si^+	$^3\Sigma^-$	−556.34581	0.27058	1.44862	0.20649
HC_8Si^+	$^1\Sigma^+$	−594.45851	0.24973	1.70405	0.25543
HC_9Si^+	$^3\Sigma^-$	−632.52660	0.26286	1.91487	0.21082
$HC_{10}Si^+$	$^1\Sigma^+$	−670.63240	0.24595	2.16340	0.24853

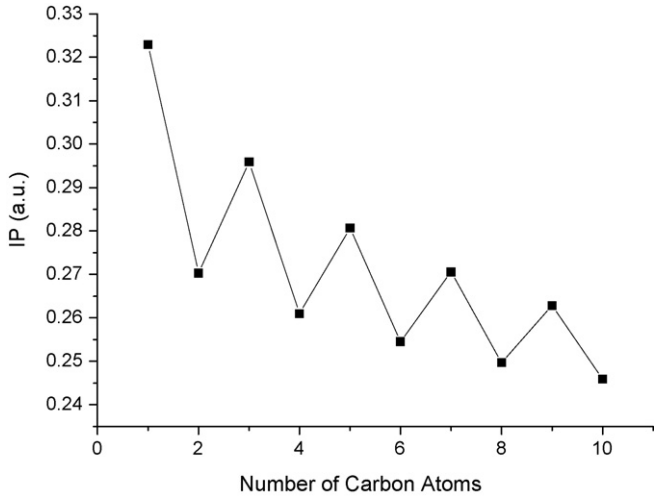

Fig. 8. Ionization potentials IP (a.u.) of the linear ground-state HC_nSi^+ (n = 1–10) clusters versus the number of carbon atoms.

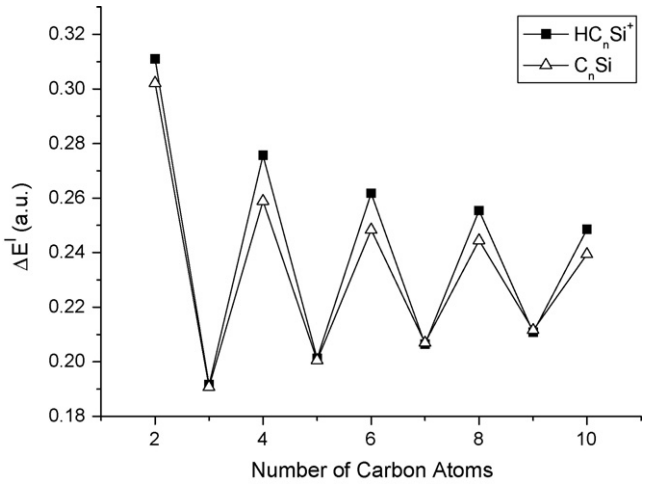

Fig. 9. Incremental binding energies ΔE^I (a.u.) of the linear ground-state HC_nSi^+ and C_nSi (n = 1–10) clusters versus the number of carbon atoms.

Ionization potentials (IP, adiabatic) are computed as the energy difference between the optimized cationic and neutral clusters ($E_{\text{optimized cation}} - E_{\text{optimized neutral}}$). A lower ionization potentials means that less energy is needed to remove an electron from the neutral molecule, and the generation of the corresponding cationic isomer is more readily done. Shown in Fig. 8 is the variation curve of ionization potentials of the most stable HC_nSi^+ (n = 1–10) versus n. One can see that the IP values of HC_nSi^+ with even n are lower than those with odd n, reflecting an alternate pattern of high and low. This implies that compared to the cases of odd n, it is easier to remove an electron from HC_nSi with even n. The pattern of odd/even alternation reiterates that the clusters with even n are more stable than those with odd n.

3.6. Incremental binding energies

The incremental binding energy (ΔE^I) which is the atomization energy (ΔE_a) difference of adjacent clusters can also be used to assess the relative stability of the cationic clusters [38]. It is expressed as

$$\Delta E^I = \Delta E_a(HC_nSi^+) - \Delta E_a(HC_{n-1}Si^+);$$

where ΔE_a is defined as the energy difference between a molecule and its component atoms [24].

Fig. 9 depicts the incremental binding energies ΔE^I (a.u.) of the linear ground-state HC_nSi^+ and C_nSi (n = 1–10) clusters versus n. As shown in Fig. 9, the values of ΔE^I of HC_nSi^+ vary according to a pattern of odd/even alternation: when n is even, the ΔE^I value is large and when n is odd, the ΔE^I is small. Because a larger ΔE^I value implies a more stable HC_nSi^+ structure, one can deduce that the even-n HC_nSi^+ clusters are more stable than the odd-n ones. Such odd/even alternation of ionization potentials (IP) and incremental binding energy is in consistency with the experimental observation [8]. It can be explained by a combined consideration of the overall behaviors of IP and ΔE^I of the clusters. Since the IP of odd-n clusters are obviously higher than that of even-n clusters, and the ΔE^I of odd-n clusters are obviously lower than that of even-n clusters, the odd-n clusters are difficult to form and more susceptible to fragmentation.

3.7. Proton affinities

Proton affinity (PA) of a molecule can be defined as the amount of energy released when a proton (H^+) is added to the molecule, and is computed as the energy difference between the molecule and the same molecule with one additional proton [24]. The PA of C_nSi can thus be related to the energy of HC_nSi^+ quantitatively as $PA = E(C_nSi) - E(HC_nSi^+)$.

Being the parent molecules of HC_nSi^+ cations, SiC_n clusters have been studied both experimentally and theoretically [7,39–54]. In the case of C_2Si, the results of some theoretical calculations suggested that the ground-state is cyclic in configuration [43,49,54]. Applying various pure and hybrid density functionals with three larger basis sets, Arulmozhiraja et al. concluded that the BLYP and B3LYP approaches failed to predict cyclic C_2Si to be more sable than linear C_2Si [42]. Also Kenny et al. carried out high-level study of C_2Si barrier to linearity, including R12 correlation methods [55]. As for C_3Si isomers, Pradhan and Ray predicted a linear ground-state structure based on both LDA and GGA to DFT investigations [49]. Employing B3LYP–DFT/6-311G(3df) to study C_3Si, Yadav et al. reported a linear SiCCC structure, and the EA (2.51 eV) calculated in this study is in good agreement with the experimental value (2.64 eV) [54]. Rintelman and Gordan studied SiC_3 using multiconfigurational self-consistent-field wave functions and considered the global minimum isomer for SiC_3 is a linear triplet with a terminal silicon atom [50]. However, the results of most HF and post-HF calculations and the results of experimental studies suggested that the ground-state of C_3Si is rhomboidal in structure [39,40,43,46,47,51,53]. According to the results of our calculations, the energy levels of linear and cyclic C_2Si are −365.563244 and −365.560480 a.u., respectively, the difference being −0.002764 a.u. (−1.735 kcal/mol). For C_3Si the total energies are −403.611271 and −403.598853 a.u. for linear and rhomboidal configurations, the difference being −0.012418 a.u. (−7.793 kcal/mol). In both cases of our studies, the nonlinear configurations are the second most stable, lying somewhat higher in energy. Based on our results of study on proton affinity (PA), such small differences in energy should not have obvious effect on the systematic characteristics of parity alternation of the HC_nSi^+ species.

Shown in Fig. 10 is a plot of the PA values of ground-state C_nSi (n = 1–10) clusters versus n; the PA values are 0.35062, 0.35949, 0.36031, 0.37703, 0.37775, 0.391164, 0.39067, 0.40164, 0.40086, and 0.40995 a.u., respectively, displaying a certain trend of relative stability of the proton-added clusters. The phenomenon can be explained in term of that with a rise in n, there is enhancement in stability of the HC_nSi^+ clusters due to a wider spread of the positive charge in the enlarged π system. It is worth pointing out that the extent of rise of PA value when C_nSi moves from odd-n to an adjacent even-n cluster is bigger than that of from even-n to

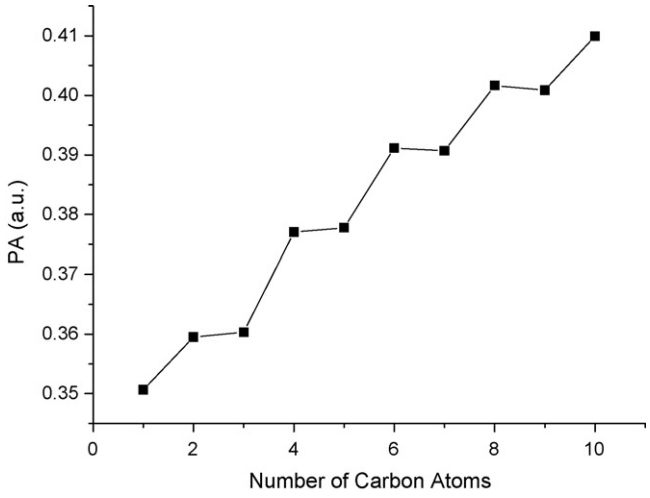

Fig. 10. Proton affinities PA (a.u.) of linear ground-state C_nSi (n = 1–10) clusters versus n.

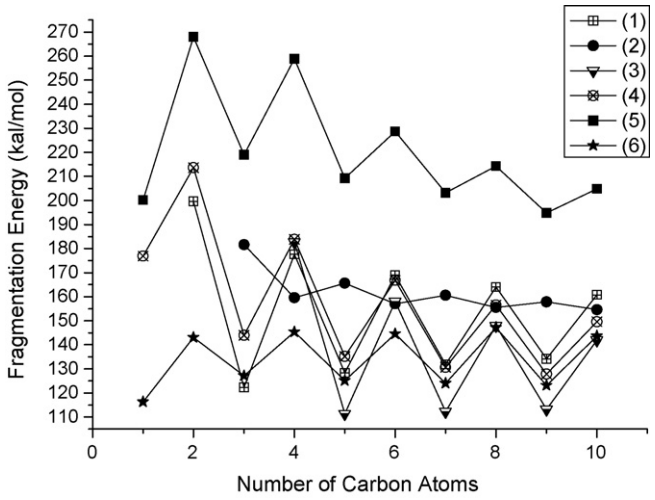

Fig. 11. Fragmentation energies (kcal/mol) versus the number of carbon atoms.

odd-n clusters. As shown in Fig. 9, the ΔE^{l} of ground-state C_nSi clusters show an odd/even alternation pattern similar to that of HC_nSi^+ clusters. When n is even, the ΔE^{l} values of C_nSi are smaller than those of HC_nSi^+ and when n is odd, the ΔE^{l} values are almost the same as those of HC_nSi^+. The structure of odd-n C_nSi clusters with nearly equivalent C—C bond lengths can be regarded as cumulene-like, with one lone pair of electrons located at the terminal carbon. The addition of H^+ at the terminal C atom and the formation of a C—H bond would not cause significant change to the cumulene-like structure close to the Si terminus, but the C—C bonds next to the H terminus displaying characters of triple bond and the C—Si bonds showing characters of single bond. The structure of odd-n C_nSi and HC_nSi^+ displayed similar ΔE^{l} values but showed slight discrepancy in PA values. When n is even, the formation of the C—H bond would result in a polyacetylene-like structure of higher stability, showing obvious alternation in C—C bond length along the C_n chain. That would be reflected in higher ΔE^{l} and larger increase in PA values.

3.8. Dissociation channels

Due to the existence of a silicon and hydrogen atom at the ends of the C_n chains, the possible dissociation channels of HC_nSi^+ (n = 1–10) could be rather complicated. It is not our intention to characterize the reaction pathways and transition states for fragmentation. Nevertheless, it is worthwhile to evaluate the relative stability of the clusters in term of fragmentation energy based on hypothetical reactions. The energies for fragmentation versus n are depicted in Fig. 11. The six dissociation channels are divided into two categories: Reactions (1)–(3) with C, C_2, and C_3 generation and Reactions (4)–(6) with Si, HSi, and H generation.

$$HC_nSi^+ \rightarrow HC_{n-1}Si^+ + C \quad (1)$$

$$HC_nSi^+ \rightarrow HC_{n-2}Si^+ + C_2 \quad (2)$$

$$HC_nSi^+ \rightarrow HC_{n-3}Si^+ + C_3 \quad (3)$$

$$HC_nSi^+ \rightarrow HC_n^+ + Si \quad (4)$$

$$HC_nSi^+ \rightarrow C_n^+ + HSi \quad (5)$$

$$HC_nSi^+ \rightarrow C_nSi^+ + H \quad (6)$$

Fragmentation energies related to Reaction (1) with the release of one carbon atom exhibits distinct odd/even alternation and the dissociation energies of HC_nSi^+ with even n are always larger than those with odd n. The results are consistent with the observation that HC_nSi^+ cationic clusters with even n are relatively more stable; the ejection of a single carbon atom will cause an inverse in parity of the clusters and the more stable "even-n" clusters requires more energy for fragmentation than the less stable "odd-n" clusters. In Reaction (2), the losing of a C_2 fragment does not cause significant change in parity of the parent anionic clusters, and the alternation effect is much less apparent than that of Reaction (1). The energy curve of Reaction (3) shows the same odd/even tendency of Reaction (1). In Reaction (3), the energy needed for dissociation is smaller than that required for Reactions (1) and (2) plausibly due to the special structural stability of the C_3 fragment as previously pointed out by Rao et al. [56]. The dissociation energy of Reactions (4)–(6) which involve the loss of Si, SiH, and H, respectively, exhibit similar odd/even alternation. Compared to Reaction (4) that involves the breaking of a Si—C bond, Reaction (5) needs more energy because there is the breaking of a Si—C as well as a C—H bond. Reaction (6) with the loss of a H fragment does not show a significant change in parity; the dissociation energy are the smallest and the loss of a hydrogen atom could be the dominant dissociation pathway. In summary, the energy needed for HC_nSi^+ (n = 1–10) clusters dissociation in Reactions (1), (3)–(6) is bigger in the cases of even n as compared to those of odd n.

4. Conclusions

The linear ground-state structures of HC_nSi^+ (n = 1–10) are linear with the Si and H atom located at the ends of the C_n chain. When n is even, the bond lengths and bond orders suggest a polyacetylene-like structure along the C_n chain, whereas when n is odd, the data suggest a structure that fades into a cumulenic-like arrangement towards the Si end. The even-n cationic clusters are more stable than the odd-n ones. The regularity of odd/even alternation are illustrated according to the properties of bond character, atomic charge, electronic configuration, the highest vibrational frequency, ionization potential, and incremental binding energy. The results are in agreement with the relative intensity of the HC_nSi^+ (n = 1–10) species observed in experimental studies.

Acknowledgements

The authors thank the National Science Foundation (Grants 20473061, 20533020, and 20423002) for financial supports.

References

[1] W. Weltner Jr., R.J. Van Zee, Chem. Rev. 89 (1989) 1713.

[2] Y.H. Le Teuff, T.J. Millar, A.J. Markwick, Astron. Astrophys., Suppl. Ser. 146 (2000) 157.
[3] T.J. Millar, Astrophys. Space Sci. Libr. 305 (2004) 17.
[4] P. Thaddeus, M.C. McCarthy, Spectrochim. Acta, Part A 57A (2001) 757.
[5] P. Thaddeus, M.C. McCarthy, M.J. Travers, C.A. Gottlieb, W. Chen, Faraday Discuss. 109 (1998) 121.
[6] F. Cataldo, Int. J. Astrobiol. 5 (2006) 37.
[7] M.C. McCarthy, A.J. Apponi, C.A. Gottlieb, P. Thaddeus, Astrophys. J. 538 (2000) 766.
[8] Q.J. Huang, Z.Y. Liu, H.F. Liu, R.B. Huang, L.S. Zheng, Chin. J. Chem. Phys. 8 (1995) 113.
[9] P. Botschwina, A. Heyl, W. Chen, M.C. McCarthy, J.U. Grabow, M.J. Travers, P. Thaddeus, J. Chem. Phys. 109 (1998) 3108.
[10] P. Botschwina, A. Heyl, M. Oswald, T. Hirano, Spectrochim. Acta, Part A 53 (1997) 1079.
[11] P. Botschwina, R. Oswald, Chem. Phys. Lett. 319 (2000) 587.
[12] A. Heyl, P. Botschwina, T. Hirano, J. Chem. Phys. 107 (1997) 9702.
[13] M.C. McCarthy, A.J. Apponi, V.D. Gordon, C.A. Gottlieb, P. Thaddeus, T. Daniel Crawford, J.F. Stanton, J. Chem. Phys. 111 (1999) 6750.
[14] M.C. McCarthy, A.L. Cooksy, S. Mohamed, V.D. Gordon, P. Thaddeus, Astrophys. J., Suppl. Ser. 144 (2003) 287.
[15] A. Scemama, P. Chaquin, M.-C. Gazeau, Y. Benilan, J. Phys. Chem. A 106 (2002) 3828.
[16] L.J. Allamandola, D.M. Hudgins, C.W. Bauschlicher Jr., S.R. Langhoff, Astron. Astrophys. 352 (1999) 659.
[17] Z.Y. Liu, Z.C. Tang, R.B. Huang, Q. Zhang, L.S. Zheng, J. Phys. Chem. A 101 (1997) 4019.
[18] J.R. Flores, J. Phys. Chem. B 107 (2003) 9711.
[19] Hypercube Inc., HyperChem Reference Manual, Waterloo, Ont., Canada, 1996.
[20] M. James, C. Crabbe, J.R. Appleyard, C.R. Lay, Desktop Molecular Modeller, Oxford University Press, Walton Street, Oxford, Great Britain, 1994.
[21] M.J. Frisch, G.W. Trucks, H.B. Schlegel, G.E. Scuseria, M.A. Robb, J.R. Cheeseman, J. Montgomery, J.A., T. Vreven, K.N. Kudin, J.C. Burant, J.M. Millam, S.S. Iyengar, J. Tomasi, V. Barone, B. Mennucci, M. Cossi, G. Scalmani, N. Rega, G.A. Petersson, H. Nakatsuji, M. Hada, M. Ehara, K. Toyota, R. Fukuda, J. Hasegawa, M. Ishida, T. Nakajima, Y. Honda, O. Kitao, H. Nakai, M. Klene, X. Li, J.E. Knox, H.P. Hratchian, J.B. Cross, V. Bakken, C. Adamo, J. Jaramillo, R. Gomperts, R.E. Stratmann, O. Yazyev, A.J. Austin, R. Cammi, C. Pomelli, J.W. Ochterski, P.Y. Ayala, K. Morokuma, G.A. Voth, P. Salvador, J.J. Dannenberg, V.G. Zakrzewski, S. Dapprich, A.D. Daniels, M.C. Strain, O. Farkas, D.K. Malick, A.D. Rabuck, K. Raghavachari, J.B. Foresman, J.V. Ortiz, Q. Cui, A.G. Baboul, S. Clifford, J. Cioslowski, B.B. Stefanov, G. Liu, A. Liashenko, P. Piskorz, I. Komaromi, R.L. Martin, D.J. Fox, T. Keith, M.A. Al-Laham, C.Y. Peng, A. Nanayakkara, M. Challacombe, P.M.W. Gill, B. Johnson, W. Chen, M.W. Wong, C. Gonzalez, J.A. Pople, Gaussian 03, Revision D.01, Gaussian, Inc., Wallingford, CT, 2004.
[22] A.D. Becke, J. Chem. Phys. 98 (1993) 5648.
[23] C. Lee, W. Yang, R.G. Parr, Phys. Rev. B: Condens. Matter 37 (1988) 785.
[24] J.B. Foresman, A. Frisch, Exploring Chemistry with Electronic Structure Methods, Gaussian, Inc., Pittsburgh, PA, 1996.
[25] G. Pascoli, H. Lavendy, Chem. Phys. Lett. 312 (1999) 333.
[26] K. Chuchev, J.J. BelBruno, J. Phys. Chem. A 108 (2004) 5226.
[27] M.D. Chen, J. Liu, Q.B. Chen, Q.E. Zhang, C.T. Au, Int. J. Mass Spectrom. 262 (2007) 136.
[28] L. Pan, B.K. Rao, A.K. Gupta, G.P. Das, P. Ayyub, J. Chem. Phys. 119 (2003) 7705.
[29] A. Dreuw, L.S. Cederbaum, J. Chem. Phys. 111 (1999) 1467.
[30] L. Largo, A. Cimas, P. Redondo, V.M. Rayon, C. Barrientos, Int. J. Mass Spectrom. 266 (2007) 50.
[31] J.R. Flores, A. Largo-Cabrerizo, J. Largo-Cabrerizo, J. Mol. Struct. (Theochem) 148 (1986) 33.
[32] A. Largo, C. Barrientos, J. Phys. Chem. 98 (1994) 3978.
[33] P. Redondo, A. Sagueillo, C. Barrientos, A. Largo, J. Phys. Chem. A 103 (1999) 3310.
[34] A. Van Orden, R.J. Saykally, Chem. Rev. 98 (1998) 2313.
[35] G. Li, Z. Tang, J. Phys. Chem. A 107 (2003) 5317.
[36] K.-H. Kim, B. Lee, S. Lee, Chem. Phys. Lett. 297 (1998) 65.
[37] S. Lee, Chem. Phys. Lett. 268 (1997) 69.
[38] G. Pascoli, H. Lavendy, Int. J. Mass Spectrom. Ion Process. 173 (1998) 41.
[39] I.L. Alberts, R.S. Grev, H.F. Schaefer III, J. Chem. Phys. 93 (1990) 5046.
[40] A.J. Apponi, M.C. McCarthy, C.A. Gottlieb, P. Thaddeus, J. Chem. Phys. 111 (1999) 3911.
[41] A.J. Apponi, M.C. McCarthy, C.A. Gottlieb, P. Thaddeus, Astrophys. J. 516 (1999) L103.
[42] S. Arulmozhiraja, P. Kolandaivel, O. Ohashi, J. Phys. Chem. A 103 (1999) 3073.
[43] M. Gomei, R. Kishi, A. Nakajima, S. Iwata, K. Kaya, J. Chem. Phys. 107 (1997) 10051.
[44] V.D. Gordon, E.S. Nathan, A.J. Apponi, M.C. McCarthy, P. Thaddeus, P. Botschwina, J. Chem. Phys. 113 (2000) 5311.
[45] R. Linguerri, P. Rosmus, S. Carter, J. Chem. Phys. 125 (2006) 034305/1.
[46] M.C. McCarthy, A.J. Apponi, P. Thaddeus, J. Chem. Phys. 111 (1999) 7175.
[47] M.C. McCarthy, A.J. Apponi, P. Thaddeus, J. Chem. Phys. 110 (1999) 10645.
[48] M.C. McCarthy, C.A. Gottlieb, P. Thaddeus, Mol. Phys. 101 (2003) 697.
[49] P. Pradhan, A.K. Ray, J. Mol. Struct. (Theochem) 716 (2005) 109.
[50] J.M. Rintelman, M.S. Gordon, J. Chem. Phys. 115 (2001) 1795.
[51] J.M. Rintelman, M.S. Gordon, G.D. Fletcher, J. Ivanic, J. Chem. Phys. 124 (2006) 034303/1.
[52] J. Robles, O. Mayorga, Nanostruct. Mater. 10 (1999) 1317.
[53] J.F. Stanton, J. Gauss, O. Christiansen, J. Chem. Phys. 114 (2001) 2993.
[54] P.S. Yadav, R.K. Yadav, S. Agrawal, B.K. Agrawal, J. Phys.: Condens. Matter 18 (2006) 7085.
[55] J.P. Kenny, W.D. Allen, H.F. Schaefer III, J. Chem. Phys. 118 (2003) 7353.
[56] B.K. Rao, S.N. Khanna, P. Jena, Solid State Commun. 58 (1986) 53.